

# A METHOD FOR CLASSIFICATION OF WIND FIELD PATTERNS AND ITS APPLICATION TO SOUTHERN CALIFORNIA

MARK C. GREEN

*Energy and Environmental Engineering Center, Desert Research Institute, Reno, NV 89506, USA*

AND

LEONARD O. MYRUP AND ROBERT G. FLOCCHINI

*Department of Land, Air and Water Resources, University of California, Davis, CA 95616, USA*

*Received 4 March 1991*

*Revised 18 July 1991*

## ABSTRACT

A method for classification of wind field patterns is described. The method forms groups of days having similar wind field patterns, including their diurnal variations. The expansion coefficients of the first eigenvector of an empirical orthogonal function analysis of the vector wind were used to determine if pairs of days are similar. A grouping procedure was then applied to form groups of similar days. Diurnally varying best-fit wind fields were generated for each group of similar days, or types. The method was applied to southern California each season for a 2-year period. Averaged mesoscale pressure and specific humidity fields were computed for each wind field pattern. Cause and effect relationships between the pressure, wind, and humidity fields in the complex topographic and meteorological setting are demonstrated.

**KEY WORDS** Wind field patterns Weather classification Empirical orthogonal function analysis

## INTRODUCTION

There have been numerous studies using varied methodologies to classify patterns of weather related variables. Most of the earlier schemes relied on an analyst to manually inspect weather maps and assign observations to a general type. McCutchan and Schroeder (1973) decided there were five basic weather patterns in southern California in the summer and assigned days based on the surface and 500 mbar pressure patterns. They then used discriminant analysis of eight variables, which resulted in reassigning some of the days to another type. This was a step toward introducing more objectivity into the classification process. More recent works have relied on automated methods for grouping observations, which removes additional subjectivity.

The use of principal component analysis (PCA) followed by cluster analysis of the factor scores has been popular in recent years (Kalkstein and Corrigan, 1986; Fujibe, 1989; Stone, 1989; Todhunter, 1989). Fujibe used a fuzzy clustering scheme, which allows for elements near the boundaries of clusters to have partial membership to neighbouring clusters. Some researchers have used a large number of meteorological variables to classify weather patterns (Stone, 1989), while others were interested in a limited number of variables, such as precipitation (Fujibe, 1989), or variables affecting the surface energy budget (Todhunter, 1989). Epperson *et al.* (1989) asserted that the potential temperature and mixing ratio are sufficient to classify air masses.

In this paper a method for classification of wind field patterns is described. In general terms, the method involved empirical orthogonal function analysis of the vector wind, similarity criteria, and a procedure for forming groups of days determined to be similar. The methodology was applied to surface winds in southern California. The main patterns, including their diurnal variations are shown and the relationship to other meteorological variables, including pressure, vertical temperature structure, and specific humidity are

0899-8418/92/020111-25\$12.50

© 1992 by the Royal Meteorological Society

demonstrated. While the methodology is applicable to any area, it was designed especially for regions with significant diurnal variation in the wind field.

The classification of wind patterns was done to support a study of the distribution of the extinction coefficient (inversely proportional to visibility) in southern California. It was hypothesized that the distribution of visibility reducing aerosols is primarily a result of meteorological conditions, especially wind field patterns. The relationship between wind field patterns and the distribution of the extinction coefficient in southern California is described in Green (1990) and Green *et al.* (1992).

### STUDY AREA AND DATA

The area of study included the southern San Joaquin Valley, the Los Angeles Basin, the Mojave Desert of California and three passes separating the Los Angeles Basin and San Joaquin Valley from the Mojave Desert. The topography of the study area is shown in Figures 1 and 2. The southern San Joaquin Valley slopes gradually upward toward the southeast and away from the valley centre; typical elevations are about 100 m. The Los Angeles Basin is less smooth, being interrupted by various hills and sloping upward toward the north-west and east; elevations range from sea-level to about 400 m. The Mojave Desert has many small, narrow mountains scattered about. Elevations on the desert floor are about 800 m in the western portion, gradually declining to less than 500 m in the eastern portion of the study area.

Major topographic features separate the three main areas. The southern Sierra Nevada range (2000–3000 m) and the Tehachapi range (1200–2000 m) separate the southern San Joaquin Valley from the Mojave Desert. The San Gabriel and San Bernardino mountains (1000–3000 m) lie between the Los Angeles Basin and the Mojave Desert.

Data were used from the locations shown in Figure 1. For each site, the name, latitude, longitude, and elevation are given in Table I. Sites 1–7 were RESOLVE data sites (Trijonis *et al.*, 1987). In addition, California Irrigation Management Information System (CIMIS) sites in the San Joaquin Valley (8–16) and South Coast Air Quality Management (SCAQMD) District data (sites 17–40) were used. Sites 41–51 were Federal Aviation Administration (FAA) airport sites. All locations had hourly wind speed and direction, and

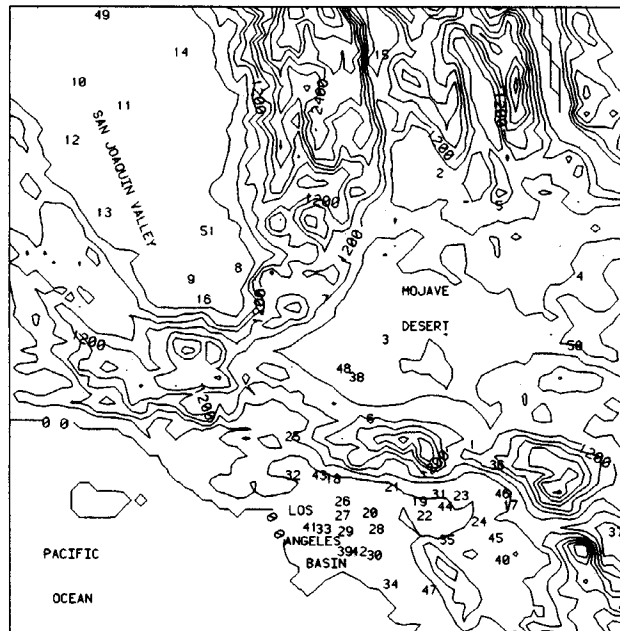


Figure 1. Topography of study area and location of data sites. Topography interval 300 m. Names of data sites are given in Table I

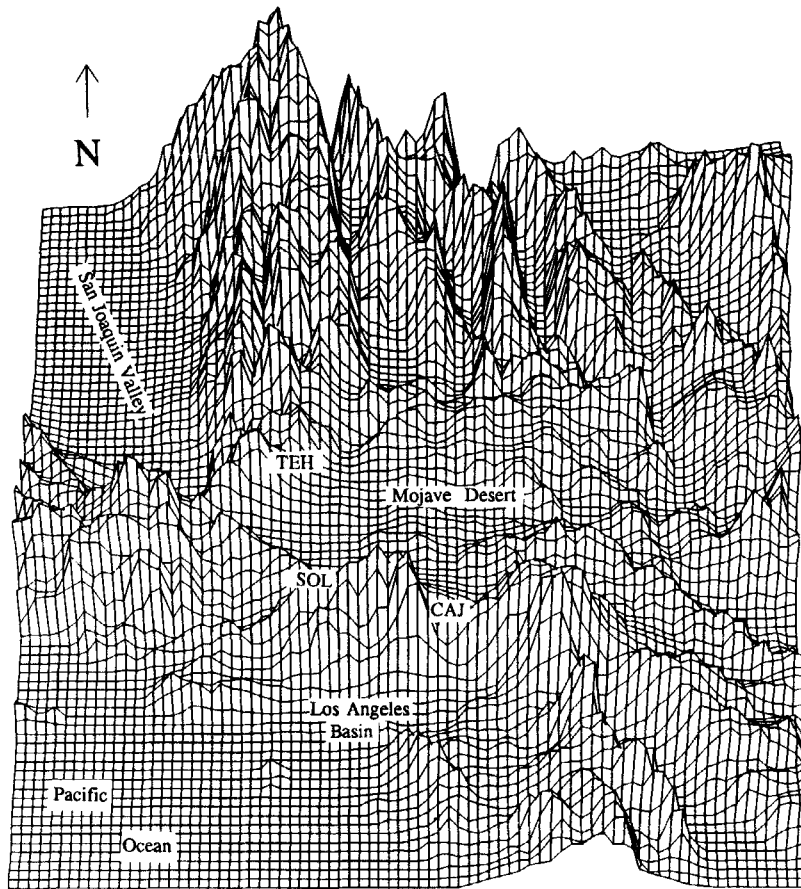


Figure 2. Three-dimensional perspective of study area, view towards the north. TEH refers to Tehachapi Pass, SOL refers to Soledad Pass and CAJ denotes Cajon pass

temperature and humidity variables, except the South Coast sites, which had wind speed and direction only. Several of the FAA sites had pressure data also. The analysis encompasses a 2-year period from September 1983 through to August 1985. Some portions of this period had a significant amount of missing data and were not studied.

### METHODOLOGY

To classify days with similar wind field patterns, an empirical orthogonal function (EOF) analysis of the vector wind was done by season. The time series expansion of the first eigenvector was used to determine similar days, followed by a grouping procedure to form groups of similar days.

The method of vector EOF analysis described by Hardy (1977) and Hardy and Walton (1978) was used. An S-mode EOF analysis of the hourly vector wind was done. In this mode, rows of the data matrix represent observations, with a column for each spatial location. The elements of the data matrix  $S$  are:

$$S_{km} \exp(i\theta_{km}) \quad m=1,M \quad k=1,N$$

where  $S_{km}$  represents the observed speed and  $\theta_{km}$  denotes the observed direction at time  $m$  and location  $k$ . A hermitian matrix  $\mathbf{H} = M^{-1}SS^{\dagger}$ , where  $S^{\dagger}$  is the complex conjugate transpose of  $S$ , is formed. Standard methods (Smith *et al.*, 1974) are used to solve  $\mathbf{H}$  for its eigenvectors (complex) and eigenvalues (real). In

Table I. Latitude, longitude and variables measured for stations with hourly data

Station	Latitude	Longitude	Variables used <sup>a</sup>
<i>RESOLVE</i>			
1. Cajon Pass	34:20:57	117:27:14	WS, WD, T, T <sub>d</sub> , RH
2. China Lake	35:42:42	117:38:58	WS, WD, T, T <sub>d</sub> , RH
3. Edwards AFB	34:52:42	117:59:31	WS, WD, T, T <sub>d</sub> , RH
4. Fort Irwin	35:12:04	116:42:38	WS, WD, T, T <sub>d</sub> , RH
5. Randsburg Wash	35:32:50	117:16:38	WS, WD, T, T <sub>d</sub> , RH
6. Soledad Pass	34:28:55	118:04:44	WS, WD, T, T <sub>d</sub> , RH
7. Tehachapi Pass	35:05:00	118:21:22	WS, WD, T, T <sub>d</sub> , RH
<i>CIMIS</i>			
8. Lamont	35:14:17	118:53:40	WS, WD, T, RH
9. Bonanza	35:09:38	119:10:51	WS, WD, T, RH
10. Stratford	36:09:27	119:51:00	WS, WD, T, RH
11. Corcoran	36:02:25	119:34:22	WS, WD, T, RH
12. Kettleman City	35:52:08	119:53:39	WS, WD, T, RH
13. Lost Hills	35:30:19	119:41:23	WS, WD, T, RH
14. Visalia	36:18:03	119:13:23	WS, WD, T, RH
15. Bishop	37:21:29	118:24:14	WS, WD, T, RH
16. Greenlee	35:04:37	119:04:52	WS, WD, T, RH
<i>SCAQMD</i>			
17. Redlands	34:03:02	117:11:10	WS, WD
18. Burbank	34:10:58	118:18:27	WS, WD
19. Pomona	34:03:60	117:44:60	WS, WD
20. Pico Rivera	34:00:53	118:03:29	WS, WD
21. Azusa	34:08:09	117:55:23	WS, WD
22. La Habra	33:59:45	117:57:07	WS, WD
23. Fontana	34:06:00	117:29:25	WS, WD
24. Riverside	33:58:10	117:22:50	WS, WD
25. Newhall	34:23:20	118:32:00	WS, WD
26. Los Angeles	34:04:02	118:13:31	WS, WD
27. Anaheim	33:59:45	118:13:50	WS, WD
28. Whittier	33:55:26	118:01:28	WS, WD
29. Lynwood	33:55:20	118:12:42	WS, WD
30. Los Alamitos	33:47:45	118:01:54	WS, WD
31. Upland	34:06:10	117:38:00	WS, WD
32. Reseda	34:11:54	118:31:49	WS, WD
33. Lennox	33:55:46	118:22:26	WS, WD
34. Costa Mesa	33:39:21	117:55:47	WS, WD
35. Norco	33:52:54	117:34:31	WS, WD
36. Lake Gregory	34:14:50	117:15:58	WS, WD
37. Palm Springs	33:49:25	116:32:27	WS, WD
38. Lancaster	34:41:38	118:08:08	WS, WD
39. Long Beach	33:49:24	118:11:19	WS, WD
40. Perris	33:46:45	117:14:31	WS, WD
<i>FAA</i>			
41. LAX	33:56:24	118:23:45	WS, WD, T, T <sub>d</sub> , RH, P
42. Long Beach	33:48:59	118:09:14	WS, WD, T, T <sub>d</sub> , RH, P
43. Burbank	34:11:58	118:21:12	WS, WD, T, T <sub>d</sub> , RH
44. Ontario	34:03:14	117:35:14	WS, WD, T, T <sub>d</sub> , RH
45. March AFB	33:53:30	117:16:30	WS, WD, T, T <sub>d</sub> , RH, P
46. Norton AFB	34:06:00	117:14:14	WS, WD, T, T <sub>d</sub> , RH, P
47. El Toro	33:37:40	117:41:25	WS, WD, T, T <sub>d</sub> , RH, P
48. W. J. Fox Field	34:44:20	118:13:10	WS, WD, T, T <sub>d</sub> , RH, P
49. Fresno	36:46	119:43	P
50. Daggett	34:52	116:47	P
51. Bakersfield	35:25	117:55	P

<sup>a</sup> WS= wind speed, WD= wind direction, T=temperature, T<sub>d</sub>=dew point temperature, RH=relative humidity, P=pressure corrected to sea level.

addition, the expansion coefficients  $c_{km}$  are complex and are given by:

$$c_{km} = E_k^\dagger \cdot S_m \quad k=1, N \quad m=1, M$$

The magnitude of the expansion coefficient represents a scaling of all eigenvector components, while the direction rotates the components through a common angle.

The input data matrix was a cross-product matrix. The ratio of the eigenvalues corresponding to a given eigenvector to the sum of all eigenvalues:

$$F_k = \frac{\lambda_k}{\sum_{j=1}^N \lambda_j} \quad k=1, \dots, N$$

gives the fraction of the energy of the wind field accounted for by that eigenvector. This ratio, which varies from 0 to 1 was dubbed the 'figure of merit' by Hardy and Walton and is analogous to the fractional reduction of variance for an EOF analysis of a covariance matrix of a scalar field.

The data was first segregated by season to remove most of the annual signal from the data. Rather than using a conventional definition of season, results of a T-mode principal components analysis of the  $u$  and  $v$  components of the monthly resultant winds for 37 locations over a 30-year period were used to group months into seasons. The input data matrix was a correlation matrix. T-mode analyses isolate subgroups of observations (months in this case) having similar spatial patterns. The analysis is described in Green (1990). The seasons were determined to be: summer, May–September; Winter, November–February; Spring, March–April; and autumn, October.

The next step was to further stratify the wind data into groups of days having similar wind field patterns. These groups of similar days will be referred to subsequently as 'types'. When developing the criteria for considering two days as similar, the objectives of the typing procedure should be considered. In addition to documenting the wind field characteristics of the area, the study was concerned with the effect of the wind field on the distribution of the extinction coefficient. Thus, the features of the wind field affecting the transport and dispersion of visibility reducing aerosols are of interest. Also, designing a typing procedure that results in a reasonable similarity of days within a type (internal cohesion), yet significant differences between types (external isolation) is desired.

The first eigenvector of the EOF analysis bears the closest resemblance to the observed data set. The time series of the expansion coefficients of the first eigenvector shows the temporal variation of the main features of the data. For every hour of each day there is an expansion coefficient associated with each eigenvector. Using the complex expansion coefficient for eigenvector 1, the wind vector at many locations and one time can be represented by a single vector. The magnitude of the expansion coefficient for eigenvector 1 equally scales all eigenvector elements and can be thought of as representing the station-wide average wind speed. The direction of the expansion coefficients rotates the eigenvector elements at all stations by a common angle and can be thought of as a wind direction.

By comparing the hourly expansion coefficients between a pair of days, the days may be considered 'similar' if differences in their expansion coefficients are within some limit. Because the diurnal variation in the wind field of the study area is known to be significant, expansion coefficients for the first eigenvector should be compared on an hourly basis for each pair of days. This will ensure that two days considered similar will have similar diurnal trends in their wind fields. The concept of determining if days are similar by comparing hourly expansion coefficients of the first eigenvector was suggested by Walton and Hardy (1978). The similarity criteria and method of grouping similar days are substantially different than those of Walton and Hardy.

Walton and Hardy considered two days similar if the magnitude of the expansion coefficients for eigenvector 1 were within 20 per cent and the direction within  $20^\circ$  for 60 per cent of the day. The grouping of similar days required these criteria to be met only for a central day and each other day in a group, but not for all pairs of days in a group. The method used in this study is described next.

Two parameters related to the average difference in magnitude and direction between two days were developed. The fractional weighted average difference in magnitude  $\Delta r_{ij}$ , is given by:

$$\Delta r_{ij} = \frac{\sum_{h=1}^{24} |r_{ih} - r_{jh}|}{\sum_{h=1}^{24} \sqrt{r_{ij} r_{jh}}}$$

where  $r_{ij}$ ,  $r_{jh}$  are the magnitude of the expansion coefficients of eigenvector 1 for days  $i$  and  $j$ , hour  $h$ . The average weighted difference in direction between two days  $\Delta\theta_{ij}$  is:

$$\Delta\theta_{ij} = \frac{\sum_{h=1}^{24} \Delta\theta_{ijh} \sqrt{r_{ih} r_{jh}}}{\sum_{h=1}^{24} \sqrt{r_{ih} r_{jh}}}$$

where  $\Delta\theta_{ijh}$  is the absolute value of the difference in direction of the expansion coefficients for hour  $h$ , days  $i$  and  $j$  and is  $\leq 180^\circ$ .

The parameters  $\Delta r_{ij}$  and  $\Delta\theta_{ij}$  give extra weight to hours with high wind speed and less weight to hours with light winds. This was done because we are interested in the transport properties of the wind field. For example, when wind speeds are low, a difference in wind direction between two days at a given hour has less effect on the transport vector than the same difference when speeds are high. Similarly an equal fractional difference in wind speed has a greater effect on transport when speeds are high. This also ensures that periods of the day with light and variable winds that may show large directional differences but little transport do not dominate the analysis.

Sensitivity analysis of the similarity criteria ( $\Delta r_{ij}$  and  $\Delta\theta_{ij}$ ) indicated a tendency for a large number of types for non-summer seasons if strict criteria were applied. Thus it was decided to use the least strict criteria that would still require reasonable similarity between days. The  $\Delta r_{ij}$  and  $\Delta\theta_{ij}$  were chosen to require that average weighted differences in direction be  $45^\circ$  and magnitude within a factor of two. It is acknowledged that this criteria are arbitrary. The  $\Delta r_{ij}$  used was 0.707; the  $\Delta\theta_{ij}$  was  $45^\circ$ .

The similarity criteria were applied to each pair of days in a season. A comparison matrix was formed indicating if each possible pair of days was similar (matrix element = 1) or not similar (element = 0). If any stations are missing for an hour, that hour cannot be used in an EOF analysis. Any days with less than 15 h of data were not included in the analysis; this criterion resulted in removal of approximately 25 per cent of the days.

Having the day comparison matrix, similar days need to be grouped. The methodology is neither straightforward nor obvious. The method is necessarily arbitrary and will affect the number and characteristics of types. However, using sound physical reasoning in developing the grouping method, the chances of useful results can be enhanced.

A distance parameter was computed for each pair of similar days. The parameter sums the magnitude of the difference in the hourly expansion coefficient for each pair of days and then normalizes by dividing by the average magnitude. The parameter is given by:

$$d_{ij} = \frac{\sum_{h=1}^{24} \sqrt{(X_{ij} - X_{jh})^2 + (Y_{ih} - Y_{jh})^2}}{\sum_{h=1}^{24} \sqrt{X_{ih}^2 + Y_{jh}^2} \sqrt{X_{jh}^2 + Y_{jh}^2}}$$

where  $X_{ih}$ ,  $X_{jh}$ ,  $Y_{ih}$ ,  $Y_{jh}$  are the  $x$  and  $y$  components of the expansion coefficients for eigenvector 1, days  $i$  and  $J$ , hour  $h$ .

The following algorithm was then used to form types:

Initially all days are untyped.

Step 1. Determine which day has the most matches (meets similarity criteria) with the pool of untyped days. Start a new type by adding this day.

Step 2. Add the untyped day most similar (least distance) to the day determined in step 1, if it matches all other days in the type.

Step 3. Repeat step 2 until all days similar to the day with the most matches (step 1) are considered.

Step 4. Go back to step 1 to begin a new type.

Step 5. Repeat the above steps until all days are typed or the remaining days match only themselves.

Step 2 limits the variability in each type by requiring all days in a type match all other days in a type. Because of this requirement, the order in which days are added to a type affects the composition of the types. This is the point in which the distance parameter is useful, by requiring the days be added sequentially in terms of least distance. Once days were assigned to groups, they remained in those groups; i.e. reclassification was not done.

This classification procedure resulted in most of the days placed in the first few groups, with a number of groups that may contain as little as 2 days. This is reasonable because some wind field patterns are rather common, while others are comparatively rare. All groups have the same allowable variation among member days. Classification methods that force the groups to be of similar size may result in some groups having a high degree of variation and other groups having little variation. In this study, it was considered most important to have internal cohesion.

Table II shows the percentage of days included in the first five types for various combinations of the similarity criteria for winter 1984–1985, the period with the most number of types. It can be seen that varying the criteria significantly affects the grouping. If wind speed requirements are loose and wind direction is restricted only to the same quadrant ( $90^\circ$ ), greater than 90 per cent of the days are contained in the first five types. For the criteria used, 51 per cent of the winter 1984–1985 days were in the first five types.

As an alternative grouping technique, the distance parameter for all possible pairs of days could have been computed and then cluster analysis used to form groups. This is being considered for future analysis.

After assigning days to types, best-fit hourly wind fields for each type are generated following the method of Walton and Hardy (1978).

## RESULTS

This section shows the results of the EOF analysis and typing process for two seasons from the 2-year period studied. Summer 1985 and winter 1984–1985 will be discussed. Other seasons are described in Green (1990).

### *Summer 1985*

The EOF analysis for summer 1985 was dominated by one eigenvector. The first eigenvector had a figure of merit of 0.64. The second eigenvector had a figure of merit of 0.10 and the third 0.05. The first eigenvector is shown in Figure 3. The magnitudes of the eigenvector elements are in non-dimensional units. The sum of the squares of the element magnitudes equals 1 for all eigenvectors. The first eigenvector is the closest approximation to the data set, averaged over all observations. Eigenvector 1 illustrates a sea-breeze flow in the Los Angeles Basin, channelled by the topographic features. Surface flow goes around either side of the San

Table II. Percentage of days included in the first five types as a function of allowable speed and direction variability within a type, winter 1984–1985

$\Delta r_{ij}$	$\Delta\theta_{ij}$ (degrees)			
	30	45	60	90
0.30	22	22	24	25
0.50	33	38	38	42
0.75	43	52	54	62
1.0	48	57	60	78
2.0	51	65	68	91

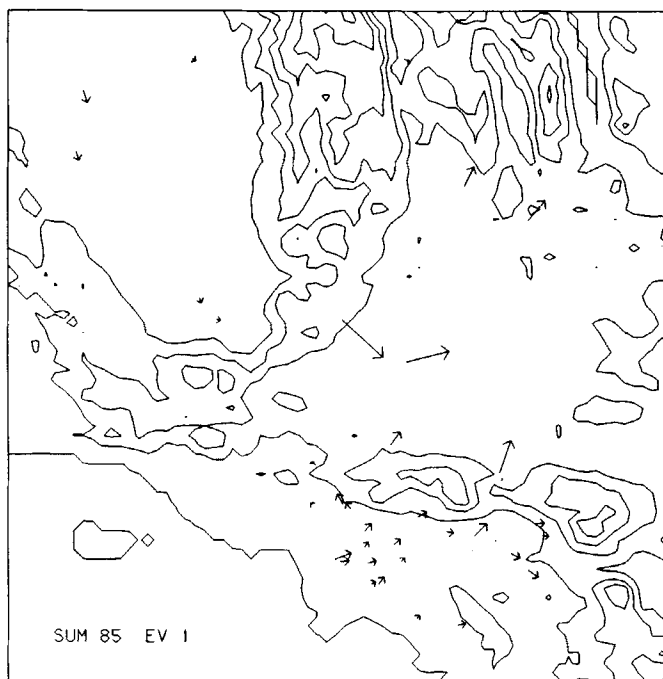


Figure 3. Summer 1985 eigenvector 1

Gabriel Mountains and over Cajon and Soledad passes into the Mojave Desert. A weak up-valley wind occurs in the San Joaquin Valley. A much stronger flow over the Tehachapi Mountains occurs at Tehachapi Pass. West to south-west flow is present at the desert locations of Edwards AFB, China Lake NWC and Randsburg Wash.

The observation vector  $\mathbf{S}$  at any time  $m$  is a linear combination of all the eigenvectors multiplied by their expansion coefficients at that time:

$$\mathbf{S}_m = \sum_{k=1}^N c_{km} \cdot \mathbf{E}_k \quad m=1, \dots, M$$

Typically, using a few eigenvectors only would closely approximate the observed data. The time series of the expansion coefficients for eigenvector 1 for a 30-day period (June 1985) is shown in Figure 4. The magnitude shown is scaled as a fraction of the maximum magnitude of the expansion coefficients. The direction is the difference from the vector sum of the coefficients (positive and negative  $180^\circ$  are equivalent). The day label corresponds to midnight at the end of a day. A regular diurnal cycle occurred in the magnitude, with a minimum typically in the late morning and a maximum in the late afternoon. The direction was very consistent, indicating little rotation of this eigenvector.

Eigenvector (EV) 2 is shown in Figure 5. As seen by the time series for EV 2 (Figure 4), there were two equally occurring directions for EV 2,  $180^\circ$  apart. The time series shows a regular cycle with a peak in the early afternoon and a secondary peak in the morning. The second eigenvector is necessary because different sites experienced phase differences in their diurnal cycles. Because the magnitude and direction at each site relative to the other sites is fixed for an eigenvector, a second eigenvector (as a minimum) is required to account for phase differences. These phase differences, especially significant for Tehachapi Pass compared with Los Angeles Basin locations, can be seen in the typical diurnal wind field patterns (shown later).

The typing process for summer 1985 resulted in five types having 64, 12, 12, 2 and 2 days. One day was untyped and 30 days had less than the 15 h of required data. The missing data seemed to be distributed randomly; one period of six consecutive days was entirely missing.

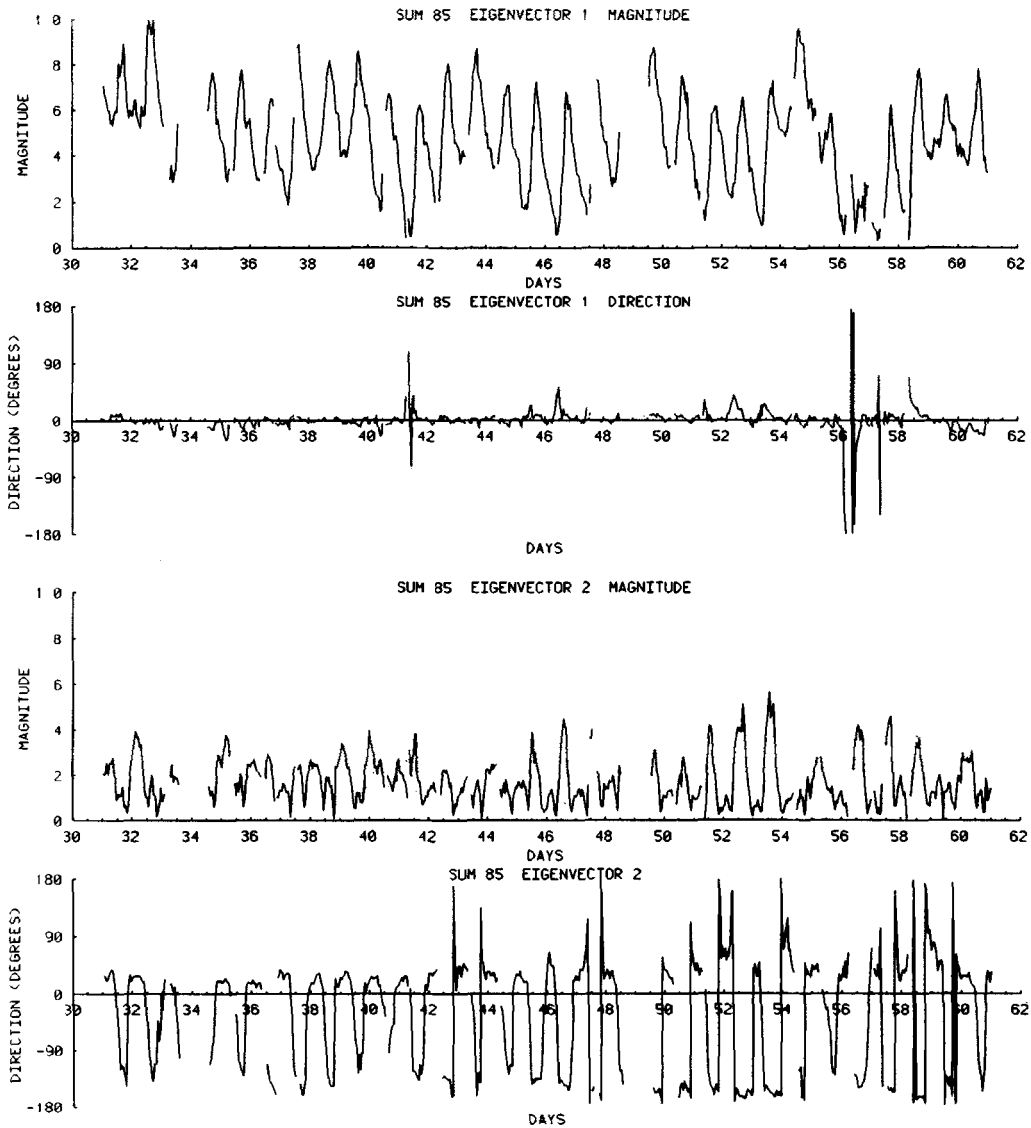


Figure 4. Summer 1985 expansion coefficients eigenvectors 1 and 2, days 32-62

The first three types will be discussed. Summer 1984 had a total of 10 types, indicating more variation in the surface wind fields. Both summers were warmer than usual. Summer 1984 was much wetter than average in the Mojave Desert owing to frequent influx of subtropical moisture; summer 1985 had virtually no precipitation, lacking the occasional thunderstorms normal in the area. Summer 1984 and 700-mbar heights were lower than normal, while summer 1985 had higher than normal heights (Ropelewski, 1985; Bergman and O'Lenic, 1986).

Wind and pressure fields at hours 8, 12, 16 and 20 (8 am, noon, 4 pm and 8 pm Pacific Standard Time) for summer 1985 type 1 are shown in Figure 6. In general, the wind flow within the Los Angeles Basin and San Joaquin Valley was shown to be from high to low pressure and proportional to the pressure gradient. These relationships, with one notable exception to be discussed later, were also true for the winds at the three pass sites; i.e. the pass winds responded to pressure gradients between the Los Angeles Basin and Mojave Desert and the San Joaquin Valley and Mojave Desert.

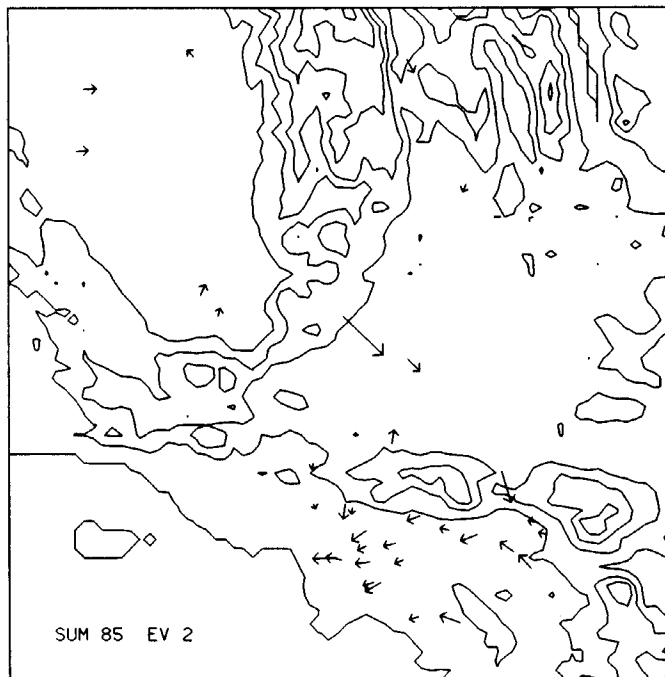


Figure 5. Summer 1985 eigenvector 2, alternative 1

At hour 8 the wind was nearly calm in the Los Angeles Basin and San Joaquin Valley, consistent with the weak pressure gradients in these areas. The three pass sites showed flow into the desert; this results from the pressure difference between the Los Angeles Basin and Mojave Desert and the San Joaquin Valley and Mojave Desert. Flow into the Mojave Desert will henceforth be termed inflow, flow out of the Mojave Desert will be called outflow.

By hour 12, a well-organized sea-breeze developed in the Los Angeles Basin as the pressure gradient across the basin increased as well as the pressure gradient between the coast and the desert. The flow across Cajon Pass increased; however, the flow through Soledad and Tehachapi passes decreased. The Soledad and Tehachapi pass stations are located on slopes on the desert side of the passes. The decrease in flow is expected to result from local pressure gradients differing from the mesoscale gradients owing to daytime heating of the slopes. When the pressure gradient across the Tehachapi range is weak, the Tehachapi site experiences outflow at hour 12, followed by inflow later in the afternoon as the San Joaquin Valley wind arrives.

At hour 16 the wind speeds were near their maximum at nearly all locations. The pressure gradients increased to 5 mbar between the coast and desert and 3 mbar between the San Joaquin Valley and desert. By hour 20 the pressure gradients all decreased, especially within the Los Angeles Basin and San Joaquin Valley; a significant gradient still existed between these areas and the Mojave Desert. At hour 24, winds within the Los Angeles Basin were nearly calm and the pressure gradients near zero; flow continued into the desert at the pass sites.

Types 2 and 3 will be discussed mainly in terms of their differences from type 1. Some general characteristics of the three types are shown in Figures 7 and 8. Figure 7 gives the daily average mesoscale pressure field for each of the types. Figure 8 shows the vertical temperature profile at hour 5 at Los Angeles.

The pressure gradients were larger for type-2 days compared with type-1 days. The Bakersfield to Daggett  $\Delta P$  averaged 5 mbar for type 2 compared with 2.7 mbar for type 1. The Los Angeles to Daggett  $\Delta P$  was slightly higher, 4.5 mb compared with 4 mbar. The 12 days in type 2 were mostly in May or early June. Type 2 included days 32, 33, 55, and 61. The expansion coefficients for these days (see Figure 4) showed a high daytime peak in magnitude and values staying higher at night than other days. Winds at Tehachapi, in

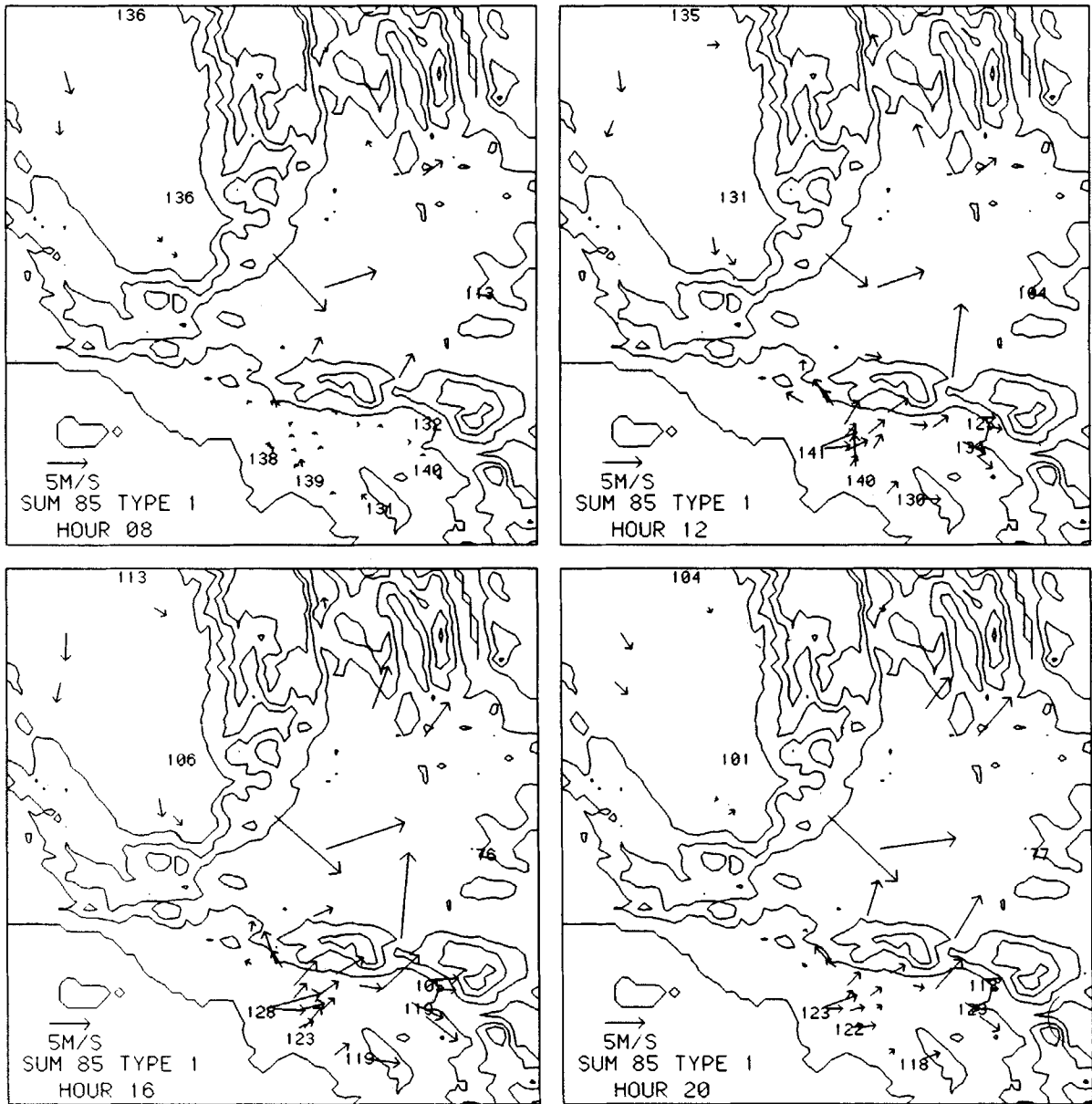


Figure 6. Wind and pressure fields summer 1985 type 1 at hours 8, 12, 16, and 20. Pressure values are the quantity (pressure adjusted to sea-level—1000 mbar) multiplied by 10

accordance with the larger  $\Delta P$  were much stronger than type 1. Other desert locations had strong winds (often  $> 10 \text{ m s}^{-1}$ ) as well. The wind and pressure for type 2 at hour 12 are shown in Figure 9. Synoptic weather maps typically showed an upper level low pressure near the west coast and a strong surface low over the four corners area. The vertical temperature profile illustrates less stable conditions for type 2. This resulted from the cold air aloft associated with the upper low over the area.

The expansion coefficients for three of the 12 type-3 days are shown in Figure 4; days 42, 47, and 58. These days had very low magnitude of the expansion coefficients during the late morning minimum and some direction fluctuation at that time. The peaks in the coefficients were similar to type-1 days.

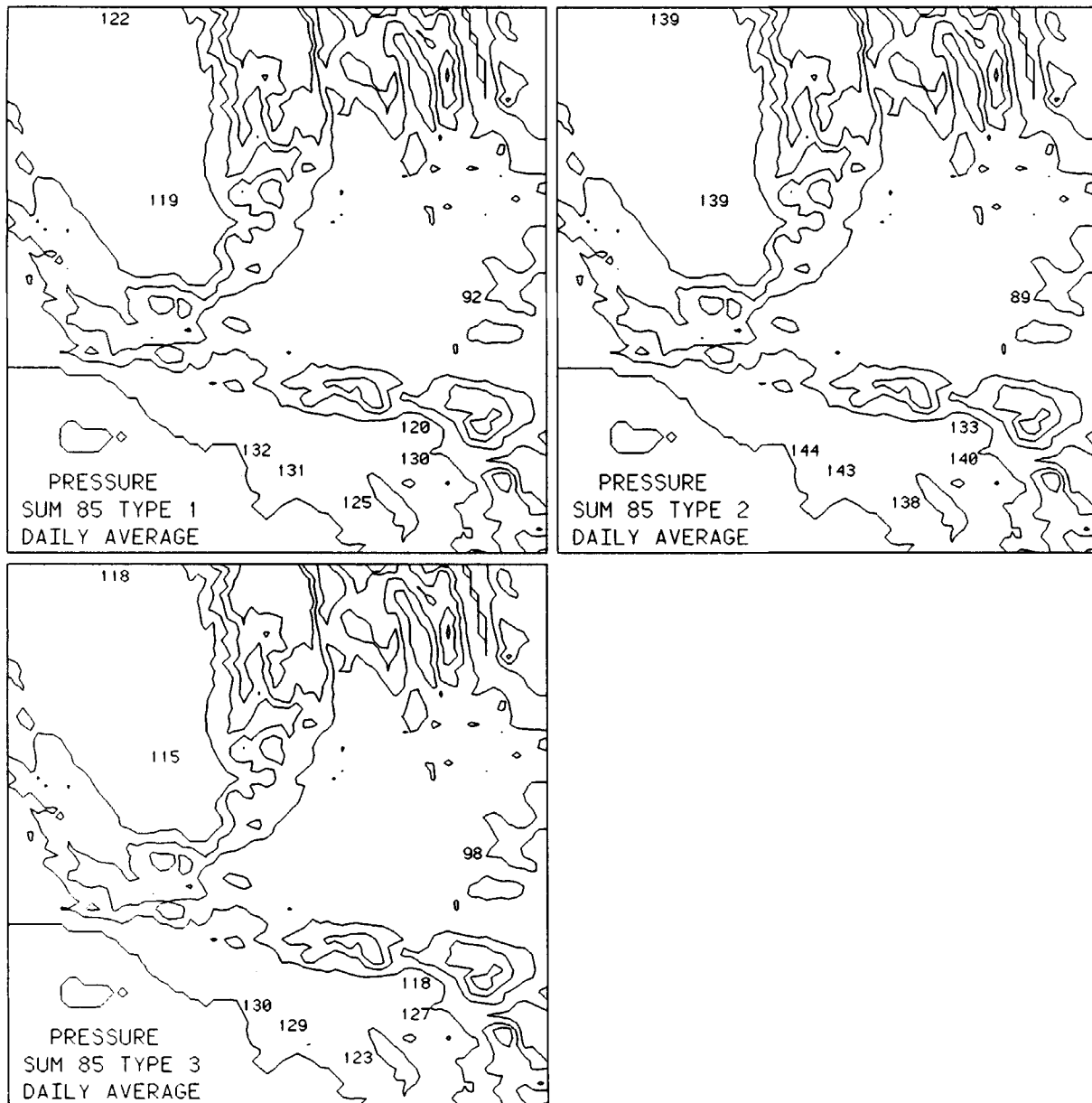


Figure 7. Pressure field summer 1985 types 1-3

Type-3 days typically had an upper level ridge inland, with the synoptic-scale surface pressure increasing toward the northeast. Pressure gradients between the San Joaquin Valley and Mojave Desert and Los Angeles Basin and Mojave Desert were less than type 1. These differences are reflected in the wind field (Figure 10). Tehachapi Pass had outflow at hour 12, and less inflow at other hours than type 1. Other sites showed less of the sea-breeze/up-valley/up-slope conditions compared with type 1, especially in the morning hours. However, the differences were most noticeable at the three pass sites.

Although the pressure gradients between the coast and Mojave Desert and San Joaquin Valley and Mojave Desert were significantly different for the three main types, the three types had very similar diurnal variations in the pressure gradients. In addition, gradients within the Los Angeles Basin were nearly identical for all three

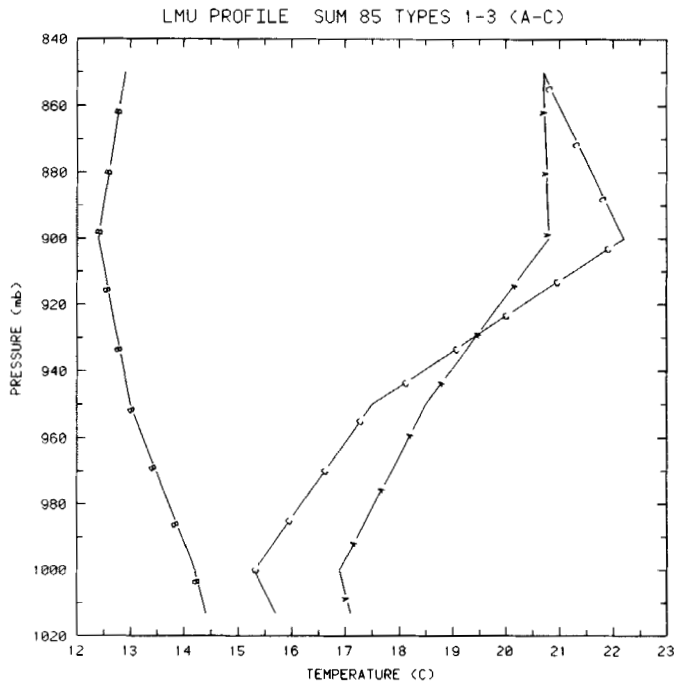


Figure 8. Vertical temperature profile at hour 5 in Los Angeles (Loyola Marymount University) summer 1985 types 1-3

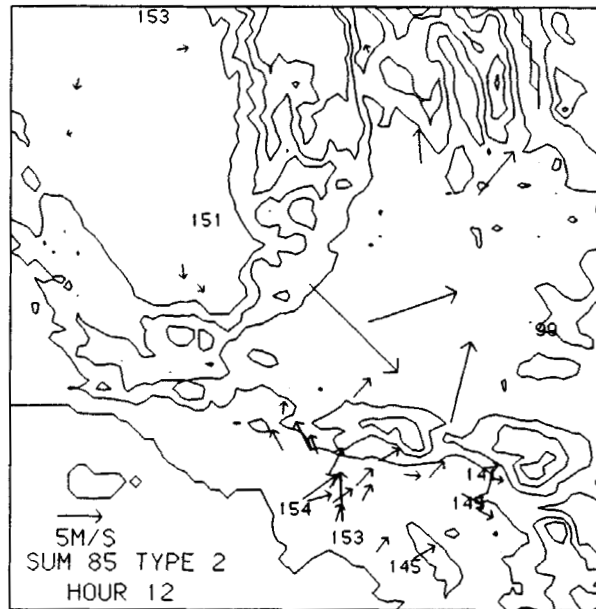


Figure 9. Wind and pressure fields at hour 12, summer 1985 type 2

types. These points can be seen in Table III, which shows the Los Angeles–Daggett and Los Angeles–San Bernardino pressure gradients at hours 8 and 16 and the difference between the hour 8 and hour 16 gradients.

These results suggest two conclusions regarding the main summer patterns: (i) increased daytime heating of inland areas compared with coastal areas adds a consistent mesoscale component to the pressure field; thus

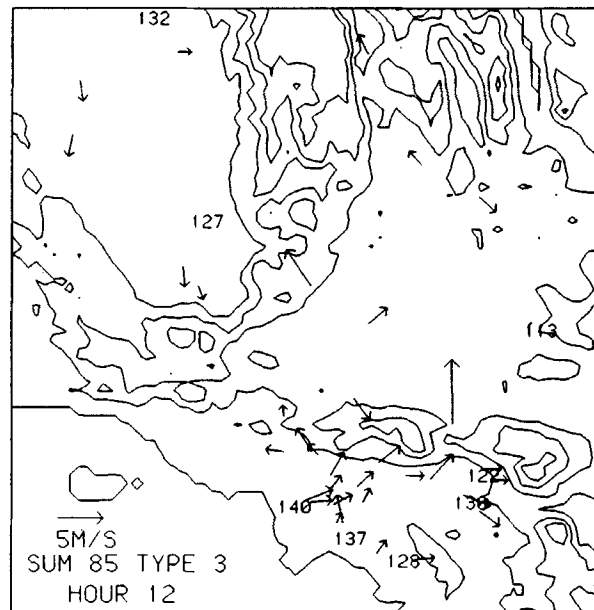


Figure 10. Wind and pressure fields at hour 12, summer 1985 type 3

Table III. Diurnal variation of Los Angeles–Daggett and San Bernardino–Daggett pressure gradients (mbar) for summer 1985 types 1–3

	Type 1			Type 2			Type 3		
Hour	8	16	16–8	8	16	16–8	8	16	16–8
LAX–DAG	2.5	5.2	2.7	4.4	7.1	2.7	1.6	3.9	2.3
SBD–DAG	1.9	2.9	1.0	3.7	4.4	0.7	1.0	1.6	0.6

the resulting mesoscale pressure field consists of a consistent mesoscale component added to a varying synoptic-scale component; and (ii) surface pressure (and surface wind) fields within the Los Angeles Basin are little affected by moderate changes in the synoptic-scale pressure field and are primarily influenced by inland versus coastal heating rates.

It was noted previously that the winds at the pass sites were affected directly by changes in synoptic-scale or cross-mountain pressure differences. It appears that the San Gabriel and San Bernardino Mountains provide enough of a physical barrier that surface pressure and wind fields in the Los Angeles Basin cannot ‘feel’ the pressure difference across the mountain barrier under typical summer conditions. This argument is not likely to be valid under Santa Ana or other strong synoptic conditions.

#### Winter 1984–1985

The EOF analysis for winter 1984–1985 was less dominated by a single eigenvector than during the summer 1985. This is to be expected owing to the greater variability in weather patterns in the winter. The first eigenvector had a figure of merit of 0.47, the second 0.19 and the third 0.07. The direction of the expansion coefficients for EV 1 showed a bimodal distribution with the two most frequent directions 180° apart. The two most frequent orientations of EV 1 are shown in Figure 11. These directions occurred with about equal frequency.

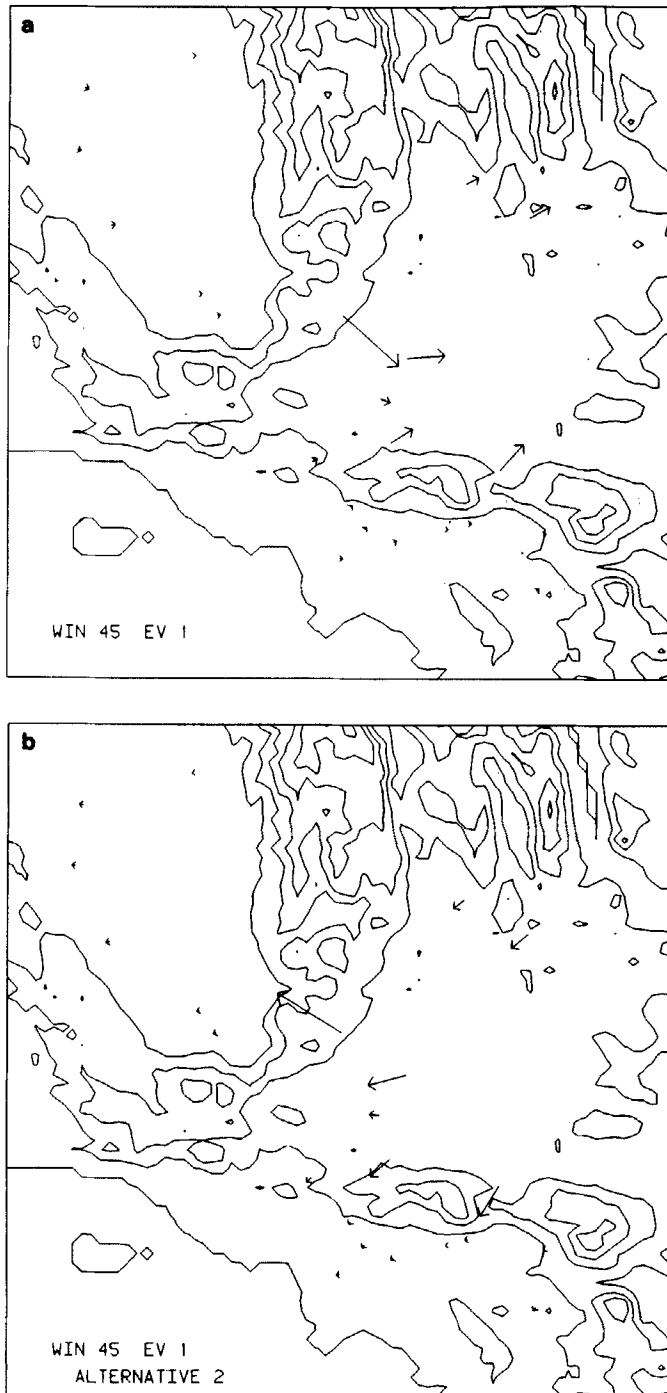


Figure 11. Winter 1984-1985 eigenvector 1. (a) Alternative 1, (b) Alternative 2

Eigenvector 2 was also bimodal. However, one mode was more frequent and had a wider angular variation. The primary mode is shown in Figure 12. Time series for one month of the period, November 1984 for EV 1 and EV 2 are shown in Figure 13. The expansion coefficients did not have the temporal regularity of the summer expansion coefficients. There was not a clear 24-h cycle as in summer; the cycles were irregular and

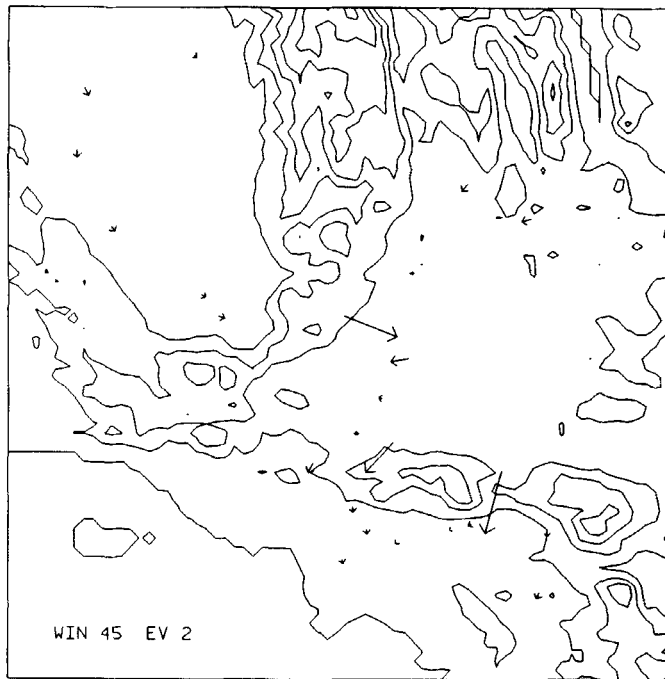


Figure 12. Winter 1984–1985 eigenvector 2, alternative 1

more typically of the order of a few days. Thus, the first two eigenvectors appear to be representing primarily synoptic-scale systems rather than mesoscale phenomena as in summer. Periods with large direction shifts and high magnitude of EV 1 expansion coefficients corresponded to frontal passages. This was apparent by looking at surface weather maps.

The first two eigenvectors were dominated by the three pass sites. The first eigenvector represents flow into or out of the Mojave Desert, depending on the orientation. The second EV accounts for times in which flow at Tehachapi Pass and the two Los Angeles Basin passes had a different relationship than represented by the first eigenvector. This can be either different flow directions (inflow at Tehachapi, outflow at the other passes, or vice versa) or just a difference in the comparative magnitude of the flows.

Of the 89 days with sufficient data, 77 were grouped into 17 types. Of the 12 days not grouped, 10 had obvious diurnal changes in the synoptic-scale pressure fields. Days with insufficient data tended to have some sites missing for 2–4 entire days. From inspection of daily weather maps, these appeared to occur more frequently during stormy conditions, causing some bias in the frequency distribution of types.

Some general features of the flow patterns were noted that allowed for classification of many types (labelled by number) into a few general types (denoted by letters) for summary purposes. General type A refers to those types with flow out from the desert at all hours of the day, except allowing for inflow at Tehachapi Pass at some hours. General type B includes types with continuous desert inflow at all three passes. During general type C, outflow at the Los Angeles Basin passes occurred during night and morning hours, followed by inflow in the afternoon. Tehachapi had inflow or both inflow and outflow on type-C days. Type S days had short-term synoptic systems affecting them, such as pre-frontal or frontal passage conditions. The summary table (see Table IV) shows the frequency of general types by seasonal period. The first three types of winter 1984–1985 were of general types A, B, and C. These three types will be described.

Type 1 consisted of 15 days. Variations of this type occurred in four other types totalling an additional 14 days. Examination of weather maps showed nearly all days with surface high pressure centred over Utah or Idaho with lower pressure toward the south-west. Figure 14 shows the wind and pressure fields at noon for type 1. Plots for all hours showed flow out from the desert at the three passes. In the Los Angeles Basin, flow

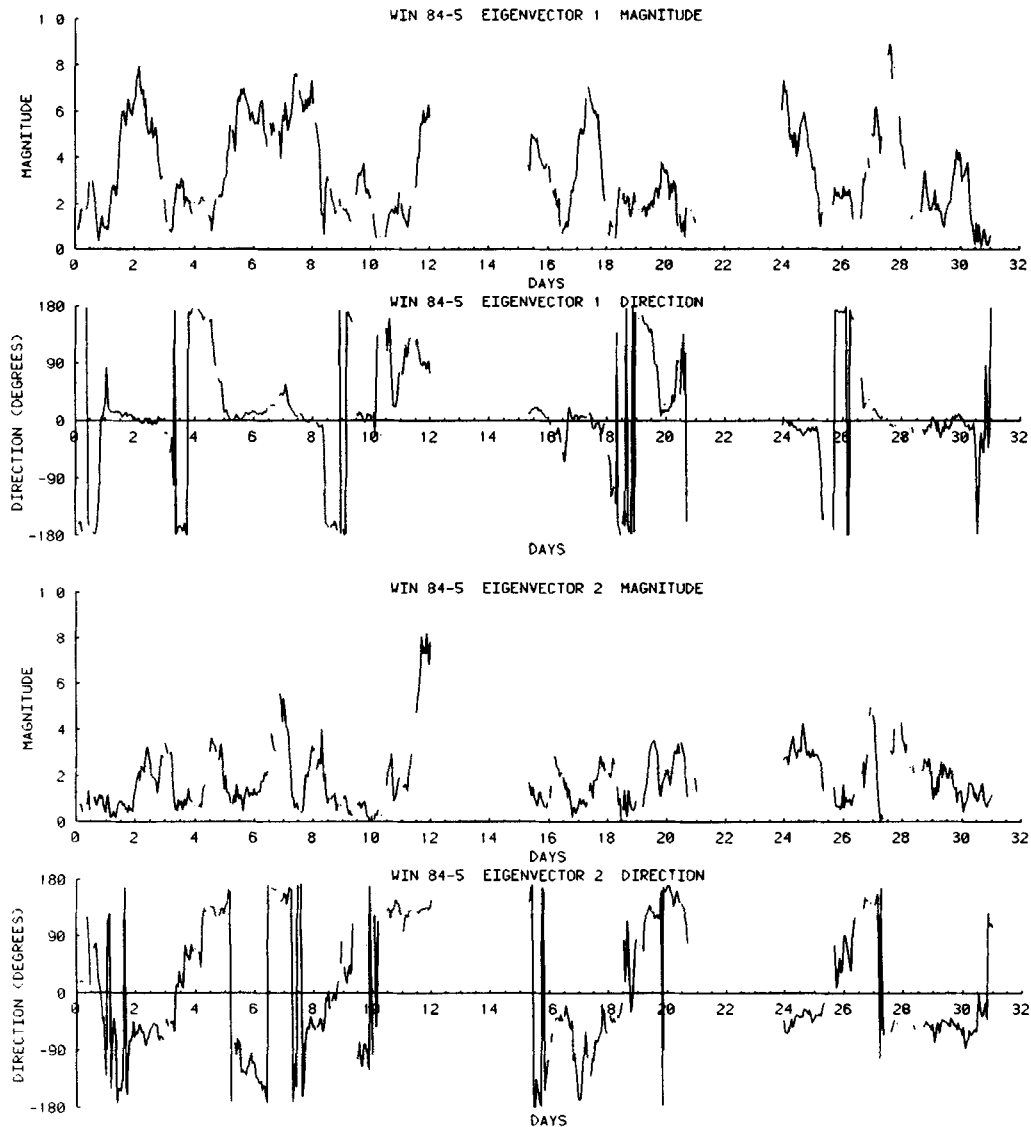


Figure 13. Winter 1984–1985 expansion coefficients eigenvectors 1 and 2, days 1–31

was offshore/down-slope except for a weak, brief onshore/up-slope flow during the mid-afternoon. The San Joaquin Valley had weak flow toward the valley centre, changing to up-valley flow in the late morning and afternoon.

The pressure patterns showed about equal pressure in the Mojave Desert and San Joaquin Valley and pressure about 3–4 mbar lower in the Los Angeles Basin. Wind flow out from the desert at 5–8  $\text{m s}^{-1}$  occurred at Cajon and Soledad passes, with the direction from high to low pressure, as is typical for these passes. At Tehachapi Pass, winds were blowing out from the desert at 8–12  $\text{m s}^{-1}$ . During the summer, it was demonstrated that the flow through Tehachapi Pass was proportional to the pressure gradient between the San Joaquin Valley and Mojave Desert. However, in this case there is virtually no pressure gradient between these areas, so there must be a different explanation for the wind. From typical surface synoptic maps, it can be seen that the flow at Tehachapi is roughly parallel to the isobars, with higher pressure to the right of the flow direction. This also can be noted from the mesoscale pressure pattern (Figure 14). This direction is



*Spring 1985*

B	16	3-6	3-3	7-5	6-5	4-4	4-2	6-4	0-31	0-31	0-31
Type 1											
Type 2	8	5-5	4-6	7-1	6-6	4-4	3-9	1-8	0	0	0
Type 3	4	3-0	1-0	7-7	7-5	4-7	4-4	5-0	0	0	0
Type 4	3	2-8	0-7	7-2	7-0	5-0	4-3	5-4	0	0	0
Type 5	3	-0-5	1-6	6-3	6-9	3-4	3-3	13-1	0	0	0
Type 6	3	2-5	5-1	6-1	5-8	4-2	3-5	2-6	0	0	0
Type 7	3	0-6	2-0	5-1	6-3	3-2	3-0	6-5	0	0	0
Type 8	2	1-3	6-5	4-3	4-2	2-7	2-1	1-5	0	0	0
Type 9	2	-2-6	-0-8	5-3	6-1	3-6	3-6	11-2	0	0	0

*Autumn 1983*

B	4	nc	nc	10-4	8-9	7-6	5-5	2-9	0	0-06	0-06
Type 1											
Type 2	4	nc	nc	10-5	8-8	6-8	5-7	7-0	0-56	0	2-0
Type 3	3	nc	nc	10-6	9-3	8-5	6-1	2-9	3-0	1-1	3-9
Type 4	3	nc	nc	7-0	9-1	4-2	4-1	14-4	0	0	0
Type 5	3	nc	nc	9-7	8-8	5-7	5-2	8-2	0	0	0
Type 6	2	nc	nc	10-4	9-1	7-1	5-6	9-0	0-25	0	0
Type 7	2	nc	nc	10-1	8-6	8-2	5-6	5-0	0	0	0

*Autumn 1984*

B	11	nc	nc	nc	nc	nc	nc	4-9	0-09	0-01	0-09
Type 1											
Type 2	4	nc	nc	nc	nc	nc	nc	5-2	0	0	0
Type 3	4	nc	nc	nc	nc	nc	nc	5-4	0	0	0
Type 4	2	nc	nc	nc	nc	nc	nc	4-1	1-75	0	0
Type 5	2	nc	nc	nc	nc	nc	nc	12-3	0	0	0

\* LAB = Los Angeles Basin, SJV = San Joaquin Valley, PAS = Tehachapi, Soledad and Cajon passes. DES = Edwards, China Lake, Randsburg Wash and Fort Irwin. nc = not calculated or unavailable.

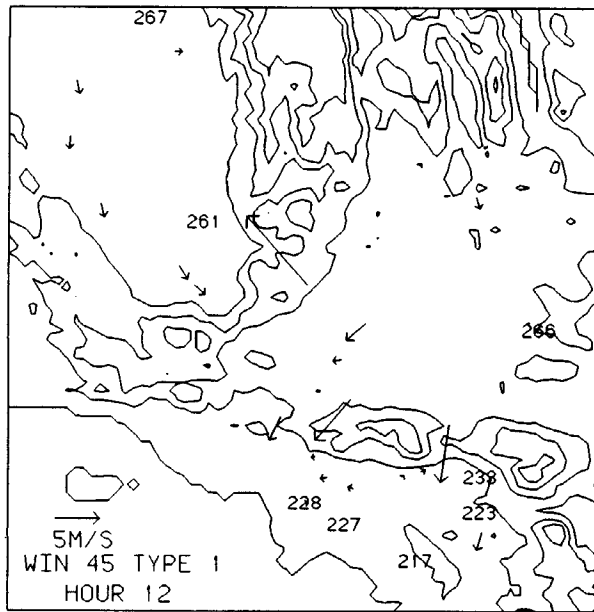


Figure 14. Wind and pressure fields at hour 12, winter 1984-1985 type 1

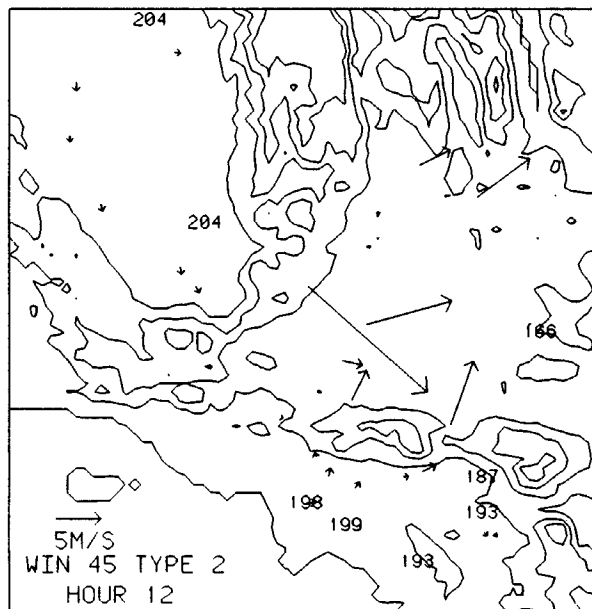


Figure 15. Wind and pressure fields at hour 12, winter 1984-85 type 2

approximately the same as would occur under geostrophic balance. However, because of the complex topography and channelling of the flow that occurred at Tehachapi Pass, it is not likely that 'balance' is occurring. Alternatively, there may be a mountain-scale pressure gradient that is on a scale less than the distance between pressure observations; one possible cause would be the damming of air at the western end of the Mojave Desert owing to flow from the north-east over the open desert. Owing to the paucity of pressure

and wind measurements in the Mojave Desert, the actual cause of the wind at Tehachapi Pass for this type is uncertain.

Type 2 consisted of 12 days. The expansion coefficients for 7 days of this type, days 2, 3, 6, 7, 18, and 25 can be seen by referring back to Figure 13. These days had a high magnitude of the coefficients with direction  $180^\circ$  from the direction for type 1 days. Wind and pressure at hour 12 for type 2 are shown in Figure 15. Flow was continuously into the desert at the three pass sites, with Tehachapi having the strongest winds, about  $15 \text{ m s}^{-1}$ . In the Mojave Desert winds were west to south-west at  $5\text{--}10 \text{ m s}^{-1}$ . The Los Angeles Basin and San Joaquin Valley had calm or nearly calm winds in the early morning and light ( $1\text{--}2 \text{ m s}^{-1}$ ) onshore and up-slope flow in the afternoon. Pressure was lower in the Mojave Desert than the Los Angeles Basin and San Joaquin Valley; Daggett pressure averaged 4.1 mbar less than Bakersfield and 3.2 mbar less than Los Angeles. In this case the wind was from high to low pressure. The daily synoptic maps showed more variation than type 1, especially at the surface. There was usually lower surface pressure to the north-east of the study area and troughing at the 500-mbar level.

The daily average specific humidity for types 1 and 2 is shown in Figure 16. All sites except China Lake had significantly higher specific humidity for type 2 compared with type 1. This indicates a difference in air masses; type 1 is continental, while type 2 is maritime.

Type 3 had 8 days. Five types, totalling 17 days, were variations of this type. This type experienced a diurnal variation of the wind and pressure gradient directions between the Los Angeles Basin and Mojave Desert. Flow was continuously into the Mojave Desert at Tehachapi, although variations of this type showed either outflow all hours or outflow in the morning and inflow in the afternoon. Daily synoptic maps showed weak pressure gradients, with this type having slightly higher pressure to the north of the study area.

Wind and pressure at hours 8, 12, 16, and 20, are shown in Figure 17. At hour 8 the pressure in the Mojave Desert was higher than in the Los Angeles Basin and within the Los Angeles Basin decreased toward the coast. Winds were light out of the desert and offshore in the Los Angeles Basin. By hour 12, the pressure in the Mojave Desert and Los Angeles Basin was nearly equal and the winds at Soledad and Cajon passes were nearly calm. Within the Los Angeles Basin, the winds became slightly onshore as the pressure gradient began to change sign. At hour 16, there was a pressure gradient of about 1 mbar between the Los Angeles Basin and

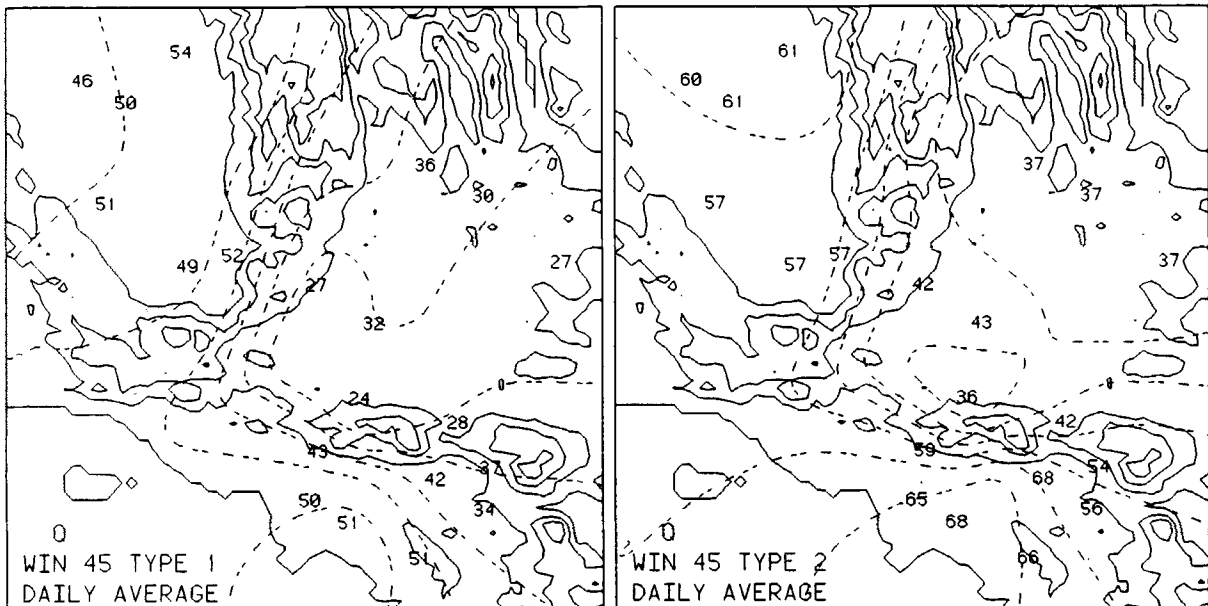


Figure 16. Daily average specific humidity fields winter 1984–1985 types 1 and 2. Numbers shown are the specific humidity multiplied by  $10^4$

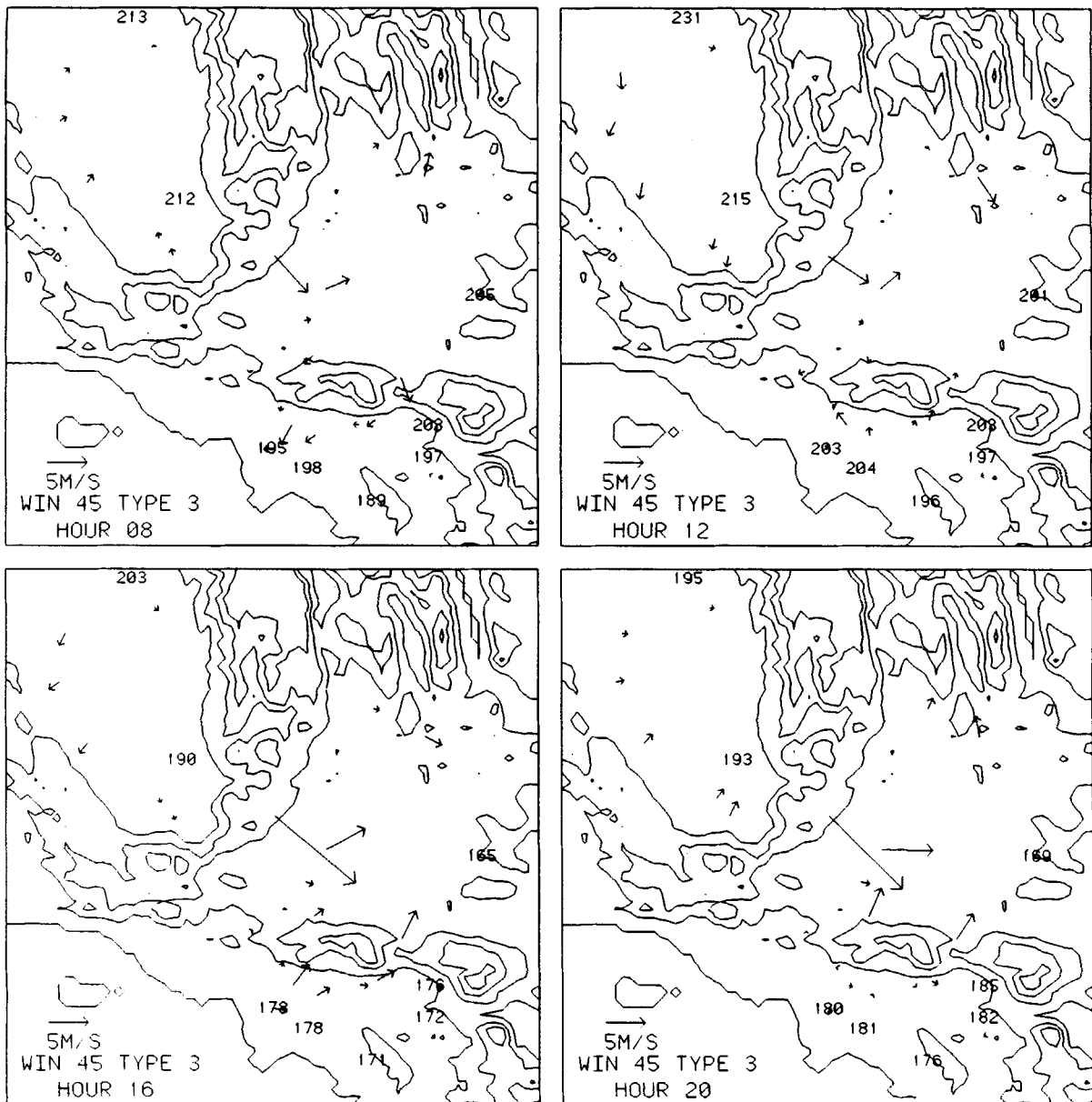


Figure 17. Wind and pressure fields winter 1984-1985 type 3 at hours 8, 12, 16, and 20

Mojave Desert and flow into the desert occurred at Cajon and Soledad passes. A weak sea-breeze occurred in the Los Angeles Basin along with a decrease in pressure from the coast inland. At hour 20 there was still a positive pressure gradient between the Los Angeles Basin and Mojave Desert and desert inflow continued at Soledad and Cajon. The pressure gradient had reversed in the Los Angeles Basin, there being a small offshore gradient. The sea-breeze had come to a stop; winds were nearly calm. It may be argued that the directional change of the pressure gradient (and friction) acted to reduce the momentum of the sea-breeze and resulted in near calm winds. It was not until after hour 24 that significant offshore/down-slope flow developed.

The pressure difference between Bakersfield and Daggett averaged about 2.5 mbar. An increase of about 1 mbar occurred between hours 12 and 16. A significant increase in the wind speed at Tehachapi accompanied

this increase in the pressure gradient. Pressure was nearly equal at Fresno and Bakersfield at hours 8 and 16 and winds in the San Joaquin Valley were light. The pressure gradient was stronger at hours 12 and 16, along with the up-valley winds.

With the exception of types influenced by strong, short-term synoptic conditions, types 1-3 represented the three main types of mesoscale patterns occurring in the winter. Fundamental and consistent relationships between the wind, pressure and humidity fields occurred among the three types. Type 1 had continuous desert outflow, type 2 had continuous desert inflow and type 3 had outflow changing to inflow at the Los Angeles Basin passes and inflow, but with lower speed, at Tehachapi Pass. These wind field patterns were consistent with the pressure and humidity fields, with type 3 being intermediate between types 1 and 2. At every location

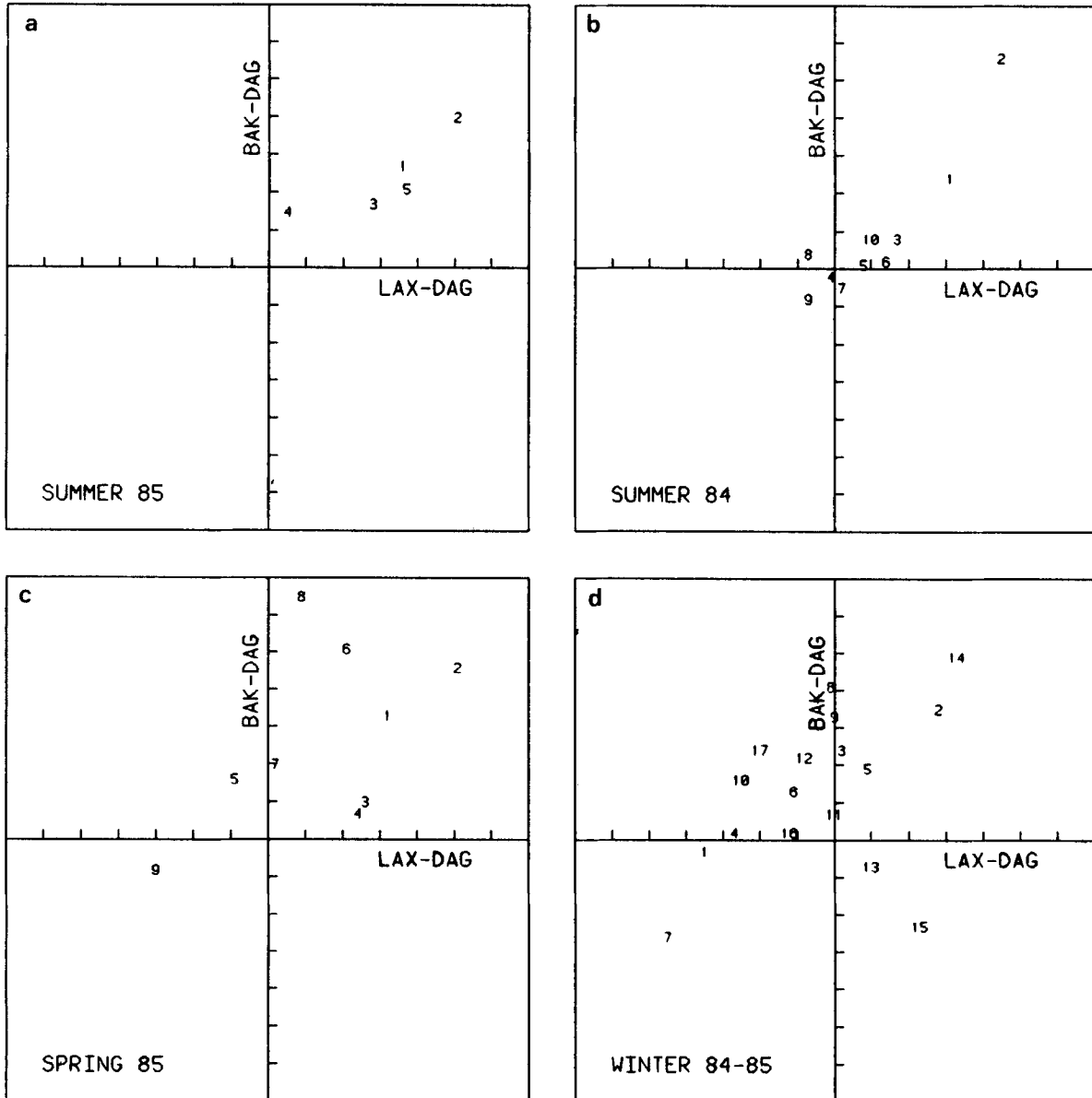


Figure 18. Daily average Los Angeles minus Daggett pressure plotted against Bakersfield minus Daggett pressure by group type. Tick marks at 1 mbar intervals. (a) Summer 1985, (b) Summer 1984, (c) Spring 1985 and (d) Winter 1984-1985

the humidity for type 3 was between the values for types 1 and 2. The other types for winter 1984–1985 are described in Green (1990).

### SUMMARY

Average daily values of various meteorological variables for each type for each season analysed are shown in Table 4. The summarized information includes: pressure gradients, specific humidity, morning vertical potential temperature gradients, the general type and number of days in each type. The values are averaged spatially over locations in each area: Los Angeles Basin, San Joaquin Valley, Mojave Desert and the passes. It should be remembered that these averages over all hours of the day and a number of locations filter out significant diurnal and spatial trends; thus the summary table tells only part of the story. The average daily pressure gradients (mbar) between Los Angeles and Daggett and Bakersfield and Daggett is shown graphically in Figure 18.

The two summers had a large majority of the days with continuous desert inflow over the passes (general type C). Winter had the lowest frequency of this general type. The intense heating of the desert coupled with the cool waters of the Pacific Ocean off California resulted in the dominance of these conditions during the summer. Summer 1984 had several types with weak pressure gradients. These types had much higher precipitation amounts than types with larger pressure gradients, with general type B days averaging 0.09 mm precipitation and general type C days averaging 0.95 mm precipitation. During the main types of the two summers, a close relationship between the 950-mbar and surface potential temperature difference at Los Angeles and the LAX–DAG pressure difference occurred, with increased stability associated with a decrease in the pressure gradient.

In winter, high pressure centres over western North America caused frequent offshore pressure gradients with continuous desert outflow (general type A). General type B patterns were frequent in the absence of significant pressure gradients and reflected diurnally reversing flows in the mountainous and coastal settings. The occurrence of synoptic (type S) conditions was most frequent in the winter. General type A conditions had low specific humidity and precipitation. General type C conditions were associated with higher specific humidity and precipitation. General type B days averaged intermediate values of precipitation and humidity.

The two autumn and one spring seasons studied had distributions of general types intermediate between summer and winter. During spring 1985, plots of the expansion coefficients of EV 1 showed a clear transition from winter to summer patterns.

In summary, the typing of weather patterns using wind fields gave consistent relationships with other variables such as synoptic and mesoscale pressure patterns, specific humidity, precipitation, and static stability. In addition, pressure and wind field relationships in southern California were demonstrated. Related studies (Green, 1990; Green *et al.* 1992) using this typing scheme illustrated cause and effect relationships between the wind field and the distribution of visibility reducing aerosols.

### ACKNOWLEDGEMENTS

Thanks to the State of California Bureau of Air Quality and Department of Water Resources, the South Coast Air Quality Management District and the Department of Defense for supplying meteorological data used in this study.

### REFERENCES

- Bergman, K. H. and O'Lenic, E. A. 1986. 'The global climate for June–August 1985—Unusually dry in several regions', *Mon. Wea. Rev.*, **114**, 2233–2254.
- Epperson, D. L., Davis, J. M., Watson, G. F. and Monahan, J. F. 1989. 'Bivariate normal classification of North American air masses using the NORMIX program', *Int. J. Climatol.*, **9**, 527–543.
- Fujibe, F. 1989. 'Short-term precipitation patterns in central Honshu, Japan: classification with the fuzzy c-means method', *J. Meteorol. Soc. Jpn.*, **67**, 967–983.
- Green, M. C. 1990. *Objective classification of wind field patterns in southern California and the relationship of these patterns to fields of the extinction coefficient, pressure and specific humidity*, PhD dissertation, University of California at Davis, 231 pp.

- Green, M. C., Myrup, L. O. and Flocchini, R. G. 1992. 'The relationship of the extinction coefficient distribution to wind field patterns in southern California', *Atmospheric Environment* (in press).
- Hardy, D. M. 1977. 'Empirical eigenvector analysis of vector observations', *Geophys. Res. Lett.*, **4**, 319–320.
- Hardy, D. M. and Walton, J. J. 1978. 'Principal components analysis of vector wind measurements', *J. Appl. Meteorol.*, **17**, 1153–1162.
- Johnson, R. A. and Wychern, D. W. 1982. *Applied Multivariate Statistical Analysis*, Prentice-Hall, Englewood Cliffs, New Jersey, 594 pp.
- Kalkstein, L. S. and Corrigan, P. 1986. 'A synoptic climatological approach for geographical analysis: assessment of sulfur dioxide concentrations', *Ann. Assoc. Am. Geogr.*, **76**, 381–395.
- McCutchan, M. H. and Schroeder, M. J. 1973. 'Classification of meteorological patterns in southern California by discriminant analysis', *J. Appl. Meteor.*, **12**, 571–577.
- Ropelewski, C. F. 1985. 'The global climate for June–August 1984—A return to normal in the tropics', *Mon. Wea. Rev.*, **113**, 1101–1106.
- Smith, B. T., Boyle, J. M., Garbow, B. S., Ikebe, Y., Klema, V. C. and Moler, C. B. 1974. 'Matrix eigenvalue routines-EISPACK guide', *Lecture Notes in Computer Science*, Vol. 6, Springer-Verlag, New York, New York.
- Stone, R. C. 1989. 'Weather types at Brisbane, Queensland: an example of the use of principal components and cluster analysis', *Int. J. Climatol.*, **9**, 3–32.
- Trijonis, J., McGown, M., Pitchford, M., Blumenthal, D., Roberts, P., White, W., Macias, E., Weiss, R., Waggoner, A., Watson, J., Chow, J. and Flocchini, R. 1987. *Visibility Conditions and the Causes of Visibility Degradation in the Mojave Desert of California*, Santa Fe Research Corp., Bloomington, Minnesota.
- Todhunter, P. E. 1989. 'An approach to the variability of urban surface energy budgets under stratified synoptic weather types', *Int. J. Climatol.*, **9**, 191–201.
- Walton, J. J., and Hardy, D. M. 1978. *Principal Components Analysis and its Application to Wind Field Pattern Recognition*, Rept. UCRL-52488, US Department of Energy, Lawrence Livermore Laboratory, Livermore, CA, 28 pp.